

Supporting Information

Non-Halogenated solvent-processed all-Polymer solar cells with efficiency of 13.8% based on a new polymer acceptor

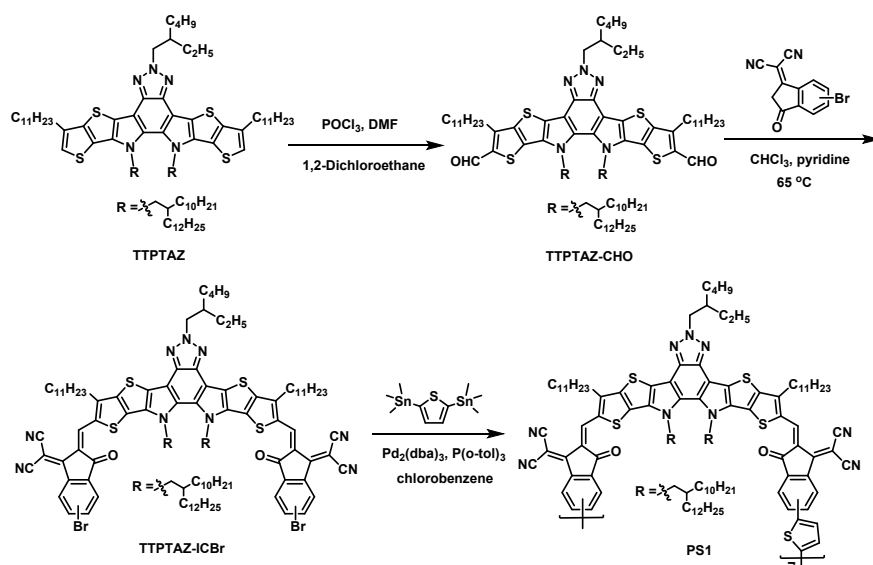
Chunguang Zhu, Zhenye Li, Wenkai Zhong, Feng Peng, Zhaomiyi Zeng, Lei Ying*, Fei Huang, Yong Cao

Institute of Polymer Optoelectronic Materials and Devices, State Key Laboratory of Luminescent

Materials and Devices, South China University of Technology, Guangzhou, 510640, China

Email: msleiyang@scut.edu.cn

1. Material and Synthesis



Scheme S1. Synthetic routes of polymer acceptor PS1.

Synthesis of PS1. All the chemical reagents were purchased from Energy Chemical, Derthon, and Alfa Aesar, and used as received directly. 2-(6-bromo-3-oxo-2,3-dihydro-1H-inden-1-ylidene)malononitrile was purchased from Derthon OPV Co Ltd; 12,13-bis(2-decyltetradecyl)-6-(2-ethylhexyl)-3,9-diundecyl-12,13-dihydro-6*H*-thieno[2'',3''-4',5']thieno[2',3':4,5]pyrrolo[3,2-*g*]thieno[2',3':4,5]thieno[3,2-*b*][1,2,3]triazolo[4,5-*e*]indole (TTPTAZ) was synthesized according to the reported literature.^{1,2}

Synthesis of TTPTAZ-CHO.

To a solution of compound TTPTAZ (1 g, 0.66 mmol) in dry 30 mL 1,2-dichloroethane and 6 mL DMF was dropped 1 mL of phosphorus oxychloride at 0 °C under the protection of nitrogen. The mixture was stirred at 0 °C for 1 h. After refluxing at 85 °C overnight, the mixture was poured into ice water (100 mL), neutralized with Na₂CO₃ (aq), and then extracted with dichloromethane. The combined organic layer was

washed with water and brine, dried over anhydrous Na_2SO_4 . After removal of solvent, the crude product was purified by silica gel using petroleum ether/dichloromethane (3:1, v/v) as eluent, yielding a light yellow liquid (0.88 g, 85 %). ^1H NMR (400 MHz, CDCl_3), δ (ppm): 10.12 (s, 2H), 4.74–4.72 (d, 2H), 4.60–4.58 (d, 2H), 3.20–3.17 (t, 4H), 2.38–2.36 (t, 1H), 1.94–1.91 (m, 6H), 1.31–0.85 (m, 141H), 0.75–0.67 (m, 6H); ^{13}C NMR (100 MHz, CDCl_3), δ (ppm): 181.59, 146.79, 142.70, 136.85, 136.52, 135.82, 132.26, 130.07, 126.29, 110.49, 59.59, 54.92, 53.42, 40.34, 38.80, 31.97, 31.93, 31.91, 30.46, 30.25, 29.77, 29.69, 29.67, 29.61, 29.57, 29.55, 29.52, 29.46, 29.42, 29.40, 29.38, 29.35, 29.32, 28.39, 28.23, 25.34, 23.95, 22.95, 22.72, 22.70, 14.15, 14.12, 14.03, 10.49. MALDI-TOF-MS: $m/z = 1570.183$ (M^+).

Synthesis of TTPTAZ-ICBr.

Compound TTPTAZ-CHO (0.50 g, 0.32 mmol) and 2-(6-bromo-3-oxo-2,3-dihydro-1H-inden-1-ylidene)malononitrile (0.30 g, 1.11 mmol) were dissolved in chloroform (60 mL). Pyridine (1 mL) was added under argon. After stirring at 65 °C overnight, the mixture was cooled to room temperature, and the solution was concentrated under reduced pressure, and poured into methanol and filtered. The crude product was purified by silica gel using petroleum ether/dichloromethane (2:1, v/v) as eluent, yielding a reddish-dark blue solid (0.54 g, 81 %). ^1H NMR (400 MHz, CDCl_3), δ (ppm): 9.18 (s, 2H), 8.85 (s, 1H), 8.58–8.56 (d, 1H), 8.03–8.02 (t, 1H), 7.87–7.85 (m, 2H), 7.79–7.77 (dd, 1H), 4.74–4.71 (t, 6H), 3.24–3.21 (t, 4H), 2.38–2.35 (t, 1H), 2.05–2.02 (m, 2H), 1.90–1.87 (m, 4H), 1.53–0.81 (m, 138H), 0.75–0.74 (m, 6H); ^{13}C NMR (100 MHz, CDCl_3), δ (ppm): 141.42, 138.54, 138.36, 137.46, 137.03, 135.48, 129.94, 129.26, 128.09,

126.61, 126.33, 124.42, 115.28, 59.72, 55.36, 40.37, 39.02, 31.97, 31.92, 31.32, 30.49, 29.94, 29.89, 29.77, 29.74, 29.72, 29.70, 29.68, 29.64, 29.57, 29.51, 29.47, 29.43, 29.36, 28.40, 26.92, 25.49, 23.99, 22.94, 22.72, 22.70, 14.13, 14.02, 10.50. MALDI-TOF-MS: $m/z = 2080.790$ (M^+).

Synthesis of polymer PS1.

Chlorobenzene (CB, 3 mL), 3 mg of $Pd_2(dba)_3$, 6 mg of $P(o-tol)_3$, 2,5-bis(trimethylstannyl)thiophene (41mg, 0.01 mmol), and TTPTAZ-ICBr (208 mg, 0.01 mmol) were added into a 10 mL flask and then protected by nitrogen atmosphere. The mixture was heated up to 120 °C and then stirred for 96 h. The reactant mixture was poured into MeOH (200 mL). The precipitate was filtered and Soxhlet extracted with methanol, acetone, hexane and chloroform. A dark solid was obtained after removing chloroform (150 mg, 75 %). GPC: $M_n = 10.9$ kDa, $M_w = 27.4$ kDa.

2. Instruments and measurements

Nuclear magnetic resonance spectra were collected on a Bruker AVANCE 500 spectrometer using tetramethylsilane (TMS) as the internal standard. MALDI-TOF-MS spectra was measured on a BrukerBIFLEXIII mass spectrometer. UV–vis absorption spectra of the NFAs samples in diluted chloroform solutions (1×10^{-5} M) and in thin films cast onto quartz glass were performed by using a HP 8453 spectrophotometer. Cyclic voltammetry (CV) experiments of NFAs thin films were carried out on an electrochemistry workstation (CHI660e, Chenhua Shanghai) using a conventional three-electrode configuration, including a Pt working electrode, a Pt wire counter

electrode, a Hg/Hg₂Cl₂ reference electrode. An anhydrous and N₂ saturated acetonitrile solution containing 0.1 M tetrabutylammonium hexylfluorophosphate (*n*-Bu₄NPF₆) was employed as the electrolyte. The Platinum stick electrode drop-coated with a thin layer of NFAs film was used as the working electrode. Differential scanning calorimetry (DSC) were recorded on a DSC214 at a heating rate of 10 °C min⁻¹ under a nitrogen flow rate of 20 mL min⁻¹. Gel Permeation Chromatography (GPC) was carried out on Agilent Technologies PL-GPC-220 at 150 °C, where 1,2,4-trichlorobenzene as the eluent and polystyrene as the standard.

The current density-voltage (*J*-*V*) characteristics were measured using a computer-controlled Keithley 2400 SourceMeter under 1 sun irradiation from an AM 1.5 G solar simulator (Taiwan, Enlitech, SS-F5). Tapping-mode AFM images were obtained by using a Bruker multimode microscope. TEM images were measured using a JEM-2100F. GIWAXS characterization was performed on MetalJet-D2 X-ray Source (Excillum). The scattering signal of was recorded on a Pilatus 3R 1M detector (Dectris) with a pixel size of 0.172×0.172 mm². The incidence angle was chosen as 0.2°, which gave the optimized signal-to-background ratio. Typically, 1800 s exposure was conducted to collect diffraction signals and two images were combined together.

3. Fabrication of PSCs

All of the solar cell devices with a conventional configuration of ITO/PEDOT:PSS/active layer/PFN-Br/Ag were fabricated. Firstly, the ITO glass substrates were pre-cleaned sequentially by using detergent, ethanol, acetone, and

isopropyl alcohol under sonication, and dried in oven at 75 °C for 6 h before to use. Followed by treating with oxygen plasma for 1 min, the PEDOT:PSS was spin-coated onto the ITO glass at 3000 rpm for 30 s and then annealed at 150 °C for 20 min in air. Subsequently, the substrates were transferred into a N₂-protected glove box for spin-coating the active layer. The donor polymer PTzBI-oF and the polymer acceptor PS1 were dissolved in CF solution or 2-MeTHF solution (with variant blend ratios, the total concentration of the donor polymer and the acceptor polymer is 5.5 mg mL⁻¹). The mixed solution was spin-coated atop the PEDOT:PSS layer at 1000 rpm for 20 s in CF or 2-MeTHF containing 1 vol% DBE to form the active layer with a film thicknesses approximately 100 nm. Then, the active layers were treated with thermal annealing at 100 °C for 10 min. Finally, the interface layer (5 nm) of PFN-Br in methanol (0.5 mg mL⁻¹) was spin-coated on the blended films, and then the top electrode silver (100 nm) was deposited onto the interlayer PFN-Br by thermal evaporation though a shadow mask in a vacuum chamber with a base pressure of 1×10⁻⁶ mbar. The active layer area of the device was 0.04 cm².

Fabrication and Characterisation of Charge-only Devices

The hole-only and electron-only mobilities of PTzBI-oF: polymer acceptors blend films and the acceptor neat films were determined from space-charge-limited current (SCLC) devices. The hole mobility was measured in a hole-only device with the configuration of ITO/PEDOT:PSS/active layer/Ag. The electron mobility was measured in an electron-only device with the configuration of ITO/ZnO/active layer/PFN-Br

Br/Ag. The ZnO sol-gel was obtained from stirring the solution of 1.0 g $\text{Zn}(\text{CH}_3\text{COO})_2 \cdot 2\text{H}_2\text{O}$ in 10 mL ethylene glycol monomethyl ether and 275 μL ethylenediamine at 60 °C for 12 h. The total concentration of PTzBI-oF and the polymer acceptor PS1 was fixed at 5.5 $\text{mg} \cdot \text{mL}^{-1}$, and the blend films were obtained by spin-coating the PTzBI-oF: PS1 (1 : 1, w/w) blend solution in CF or 2-MeTHF containing 1 vol% DBE to obtain active layer of with a film thicknesses approximately 107 nm. The mobilities were determined by fitting the dark J - V current to the model of a single carrier SCLC which were calculated on the basis of the following equation:

$$J = (9/8) \epsilon_0 \epsilon_r \mu V_{\text{eff}}^2 / d^3$$

where J is the current density, μ is the charge (hole or electron) mobility at zero field, ϵ_0 is the permittivity of free space, ϵ_r is the relative permittivity of the material, d is the thickness of the active layer, and V_{eff} is the effective voltage ($V - V_{\text{bi}}$). The charge (hole or electron) mobility was calculated from the y intercept of the J - V curves.

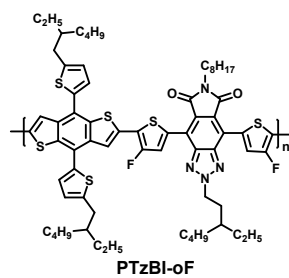


Fig. S1 Chemical structure of PTzBI-oF.

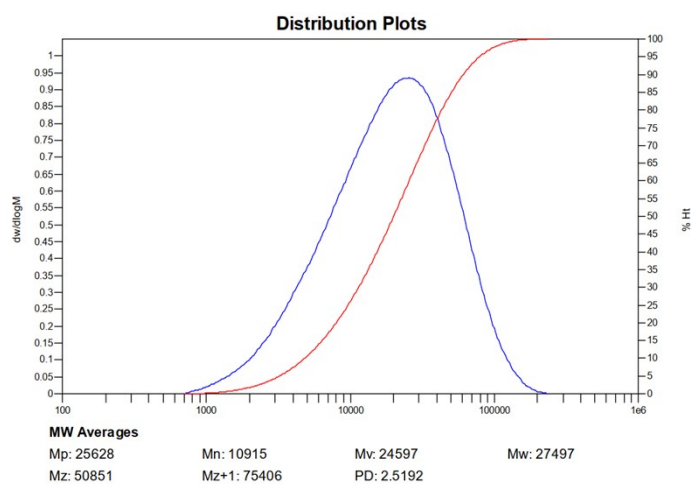


Fig. S2 GPC measurement of PS1.

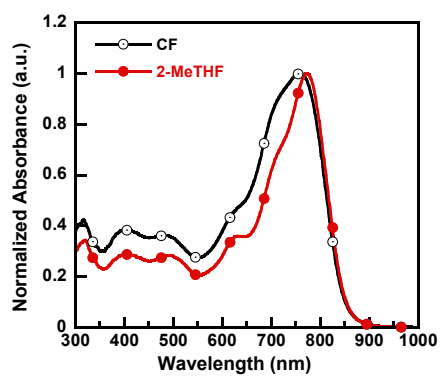


Fig. S3 Normalized UV-vis absorption spectra of PS1 in CF or 2-MeTHF solution.

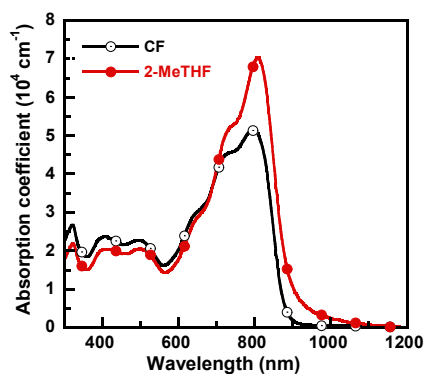


Fig. S4 Molar extinction coefficient of PS1 in thin film processed by CF or 2-MeTHF.

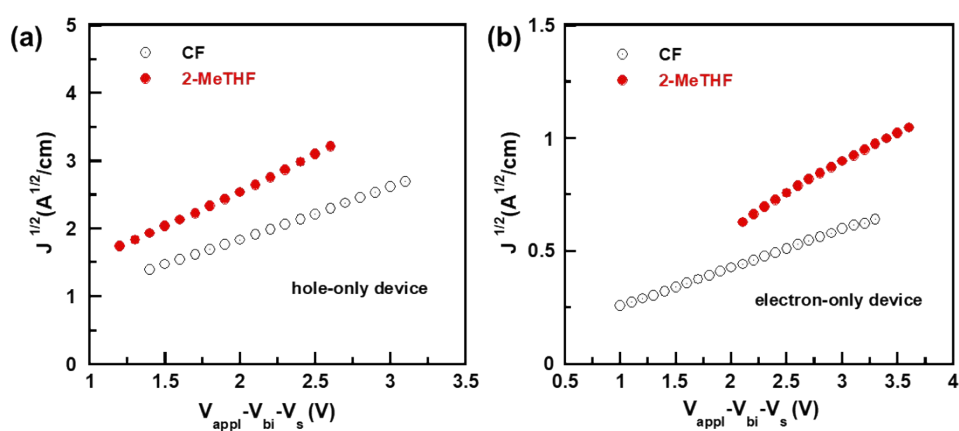


Fig. S5 (a) SCLC hole mobility for PTzBI-oF:PS1 processed by CF or 2-MeTHF; (b) SCLC electron mobility for PTzBI-oF:PS1 processed by CF or 2-MeTHF.

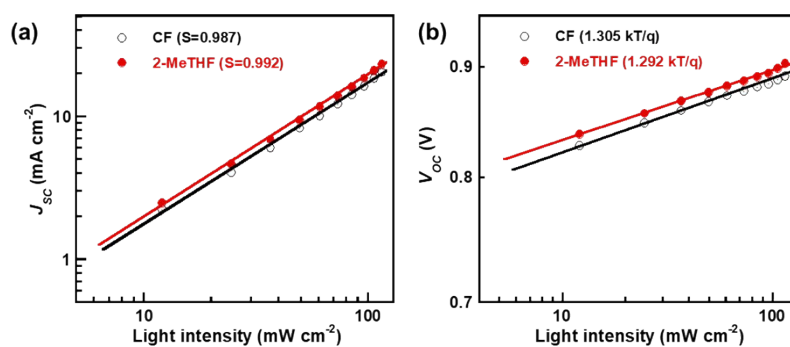


Fig. S6 (a) J_{sc} versus light intensity, (b) V_{oc} versus light intensity (P_{light}) characteristics PSCs based on PTzBI-oF:PS1 processed by CF or 2-MeTHF.

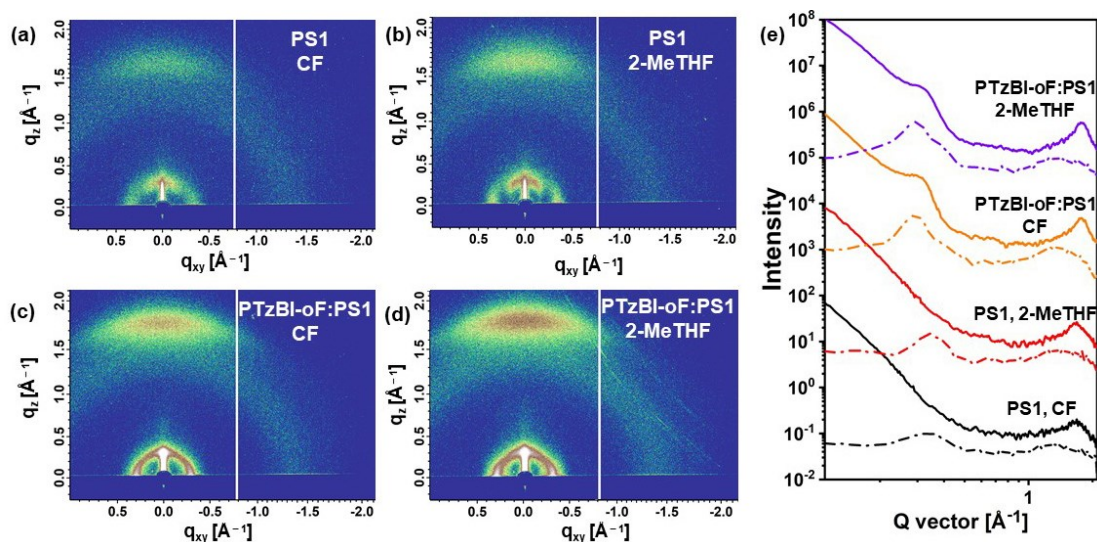


Fig. S7 2D GIWAX patterns of PS1 neat films processed by CF (a), 2-MeTHF (b) and PTzBI-oF:PS1 blend films processed by CF (c), 2-MeTHF (d) under the optimum conditions. (e) Integrated scattering profiles for the corresponding 2D patterns; the solid and dashed lines represent the OOP and IP scattering, respectively (color online).

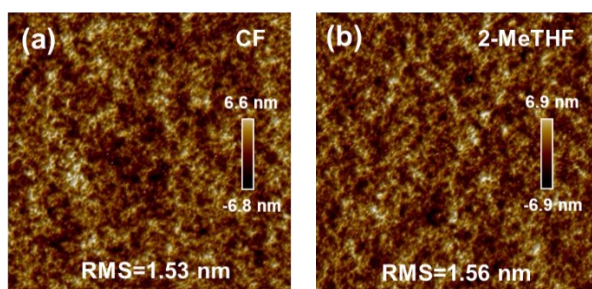


Fig. S8 AFM height images ($5 \times 5 \mu\text{m}$) of PTzBI-oF:PS1 blend films processed by CF (a), and 2-MeTHF (b).

Table S1. Summary of fused-aromatic-ring-constructed polymer acceptors for all-PSCs in the literature.

Acceptor	Donor	V_{oc} (V)	J_{sc} (mA cm ⁻²)	FF (%)	PCE (%)	Processed solvent	Ref.
PZ1	PBDB-T	0.83	16.05	68.99	9.19	CF	3
PZ1	PM6	0.96	17.1	68.2	11.2	CF	4
PN1	PM6	1.00	15.2	69	10.5	CB	5
PFBDT- IDTIC	PM6	0.97	15.39	69	10.3	CF	6
PF2-DTSi	PM6	0.99	16.48	66.1	10.77	CF	7
PT- IDTTIC	PM6	0.97	17.96	67	12.06	CF	8
A701	PBDB-T	0.92	18.27	64.0	10.70	CF	9
PF3- DTCO	PM6	0.94	15.75	68.2	10.13	CF	10
PF1-TS4	PM6	0.98	15.04	58.5	8.63	CF	11
PJ1-H	PBDB-T	0.90	22.3	70	14.4	CF	12
PYT _M	PM6	0.93	21.78	66.33	13.44	CF	13
PYE20	PBDB-T	0.905	20.97	71.73	13.60	CF	14
L14	PM6	0.96	20.6	72.1	14.3	CF	15
PTPBT- ET _{0.3}	PBDB-T	0.899	21.33	65.3	12.52	CF	16
PG1	PBDB-T	0.94	17.8	69.0	11.5	CF	17
PF5-Y5	PBDB-T	0.946	20.65	74.0	14.45	CB	18
PS1	PTzBI-oF	0.92	21.45	61.36	12.1	CF	This work
PS1	PTzBI-oF	0.92	22.47	66.70	13.8	2-MeTHF	This work

Table S2. Photophysical and electrochemical properties of the polymer acceptor PS1.

acceptor	M_n (kDa)	PDI	$\lambda_{f, \max}^a$ [nm]	$\lambda_{f, \text{onset}}^a$ [nm]	$E_g^{\text{opt } b}$ [eV]	$\epsilon_{f, \max}^c$ (cm^{-1})	HOMO [eV]	LUMO [eV]
PS1	10.9	2.52	811	893	1.39	7.04	-5.56	-3.70

^a Absorption maximum in film processed with 2-MeTHF. ^b $E_g = 1240/\lambda_{\text{onset}}$. ^c Coefficient of the polymer films processed with 2-MeTHF and the unit is 10^4 cm^{-1} .

Table S3. Photovoltaic parameters of PTzBI-oF:PS1-based all-PSCs with the active layers processed by various solvent and solvent additives under AM 1.5 G at 100 mW cm⁻².

Solvent	Solvent additive	V_{oc} (V)	J_{sc} (mA cm ⁻²)	FF (%)	PCE (%)
CF	N/A	0.940	16.58	44.21	6.89
	1% ODT	0.928	20.50	55.26	10.51
	2% ODT	0.914	21.01	61.74	11.85
	0.5% DBE	0.916	20.89	59.83	11.45
	1% DBE	0.916	21.45	61.36	12.05
	2% DBE	0.914	20.56	60.99	11.46
	2-MeTHF	N/A	0.899	21.80	62.10
0.5% CN		0.921	18.60	61.71	10.57
0.5% DBE		0.906	22.43	66.47	13.51
1% DBE		0.918	22.47	66.70	13.75
2% DBE		0.915	20.05	67.32	12.35
1% ODT		0.905	21.45	62.36	12.10

Table S4. Photovoltaic parameters of all-PSCs with thermal annealing (TA) for 10 min at different temperatures under AM 1.5 G at 100 mW cm⁻².

Device	Thermal annealing	V_{oc} (V)	J_{sc} (mA cm ⁻²)	FF (%)	PCE (%)
CF	100 °C/10min	0.916	21.45	61.36	12.05
	110 °C/10min	0.915	21.00	60.49	11.62
	120 °C/10min	0.911	20.76	60.04	11.35
2-MeTHF	100 °C/10min	0.918	22.47	66.70	13.75
	110 °C/10min	0.915	22.05	65.43	13.20
	120 °C/10min	0.911	21.78	64.79	12.85

Table S5. Photovoltaic parameters of all-PSCs with different thickness under AM 1.5 G at 100 mW cm⁻².

Device	Thickness (nm)	V _{oc} (V)	J _{sc} (mA cm ⁻²)	FF (%)	PCE (%)
CF	100	0.917	20.94	62.03	11.91
	120	0.916	21.45	61.36	12.05
	160	0.910	21.41	57.87	11.21
	200	0.905	20.83	53.76	10.13
2-MeTHF	100	0.913	21.95	67.89	13.61
	120	0.918	22.47	66.70	13.75
	160	0.910	22.40	64.98	13.25
	200	0.907	21.67	61.75	12.18

Table S6. SCLC electron (hole) mobility measurements for PTzBI-oF:PS1 films processed by CF or 2-MeTHF.

Solvent ^a	μ _h (cm ² V ⁻¹ s ⁻¹)	μ _e (cm ² V ⁻¹ s ⁻¹)	Thickness (nm)
CF	1.29×10 ⁻³	1.56×10 ⁻⁴	107
2-MeTHF	2.45×10 ⁻³	3.57×10 ⁻⁴	108

^a All of the blend films were processed by CF or Me-THF containing 1 vol% DBE and treated with 100 °C for 10 min.

Table S7. Relevant parameters obtained from $J_{\text{ph}}-V_{\text{eff}}$ curves.

Solvent ^a	$J_{\text{SC, EQE}}^{\text{b}}$ (mA cm ⁻²)	J_{ph}^{c} (mA cm ⁻²)	J_{sat} (mA cm ⁻²)	$P(E, T)^{\text{c}}$	L (nm)
PTzBI-oF:PS1	20.49	20.90	23.04	90.7%	~127
PTzBI-oF:PS2	21.21	22.78	24.27	93.9%	~126

^a All of the blend films were treated with 100 °C for 10 min ; ^b Obtained from the integration of EQE spectra; ^c At the condition of $V_{\text{eff}} = V_0 \ominus V_{\text{appl}}$ ($V_{\text{appl}} = 0$, under short-circuit condition).

Table S8. Summary of the binary all-PSCs with PCE above 10% in the literature.

Year	Acceptor	Donor	V_{oc} (V)	J_{sc} (mA cm ⁻²)	FF (%)	PCE (%)	Processed solvent	Ref.
2017	N2200	PTzBI-Si	0.865	15.76	73.76	10.1	MeTHF	19
2019	PZ1	PM6	0.96	17.1	68.2	11.2	CF	4
2019	PN1	PM6	1.00	15.2	69	10.5	CB	5
2019	BSS10	PBDB-T	0.86	18.55	64	10.1	CB	20
2019	N2200	PTzBI-Si	0.85	16.5	77.9	11.0	CPME	21
2019	N2200	PTzBI-Si	0.88	17.62	75.78	11.76	MeTHF	22
2019	PFBDT- IDTIC	PM6	0.97	15.39	69	10.3	CF	6
2020	DCNBT- TPIC	PBDTTT- E-T	0.70	22.52	64.8	10.22	CF	23
2020	PF2-DTSi	PM6	0.99	16.48	66.1	10.77	CF	7
2020	PT- IDTTIC	PM6	0.97	17.9 ¹⁶	67	12.06	CF	8
2020	A701	PBDB-T	0.92	18.27	64.0	10.70	CF	9
2020	PF3- DTCO	PM6	0.94	15.75	68.2	10.13	CF	10
2020	PJ1-H	PBDB-T	0.90	22.3	70	14.4	CF	12
2020	PYT _M	PM6	0.93	21.78	66.33	13.44	CF	13
2020	PYE20	PBDB-T	0.905	20.97	71.73	13.60	CF	14
2020	L14	PM6	0.96	20.6	72.1	14.3	CF	15
2020	PTPBT- ET _{0.3}	PBDB-T	0.899	21.33	65.3	12.52	CF	16
2020	PG1	PBDB-T	0.94	17.8	69.0	11.5	CF	17
2020	PF5-Y5	PBDB-T	0.946	20.65	74.0	14.45	CB	18
	PS1	PTzBI-oF	0.92	21.45	61.36	12.1	CF	This work

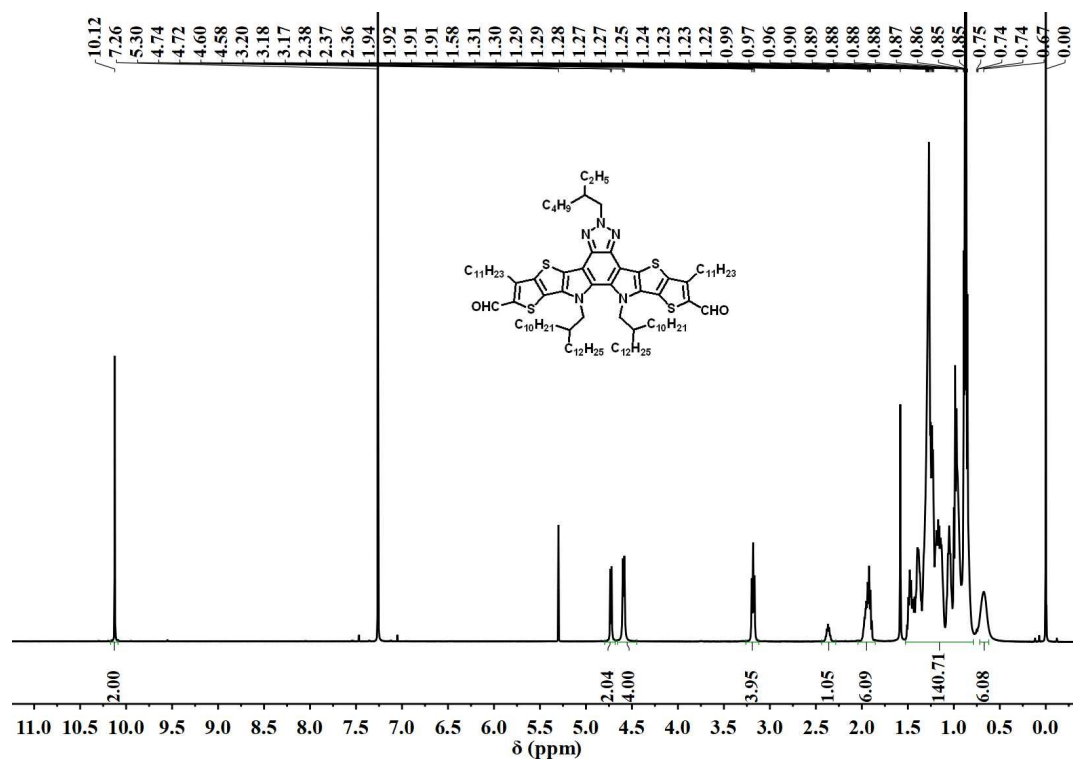


Fig. S9 ¹H NMR spectrum of compound TTPTAZ-CHO in CDCl₃.

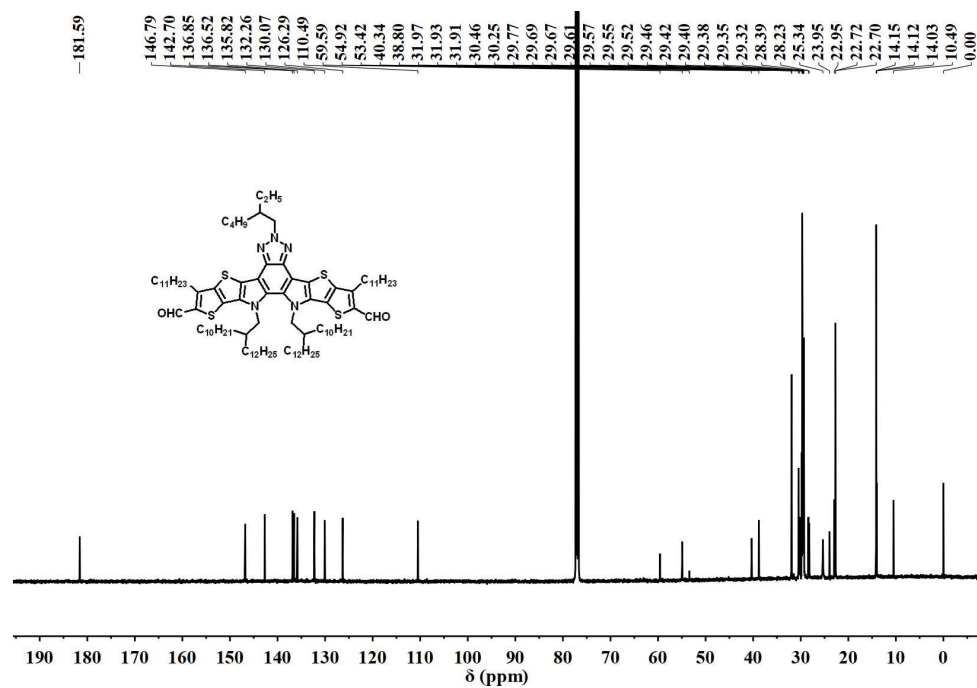


Fig. S10 ^{13}C NMR spectrum of compound TTPTAZ-CHO in CDCl_3 .

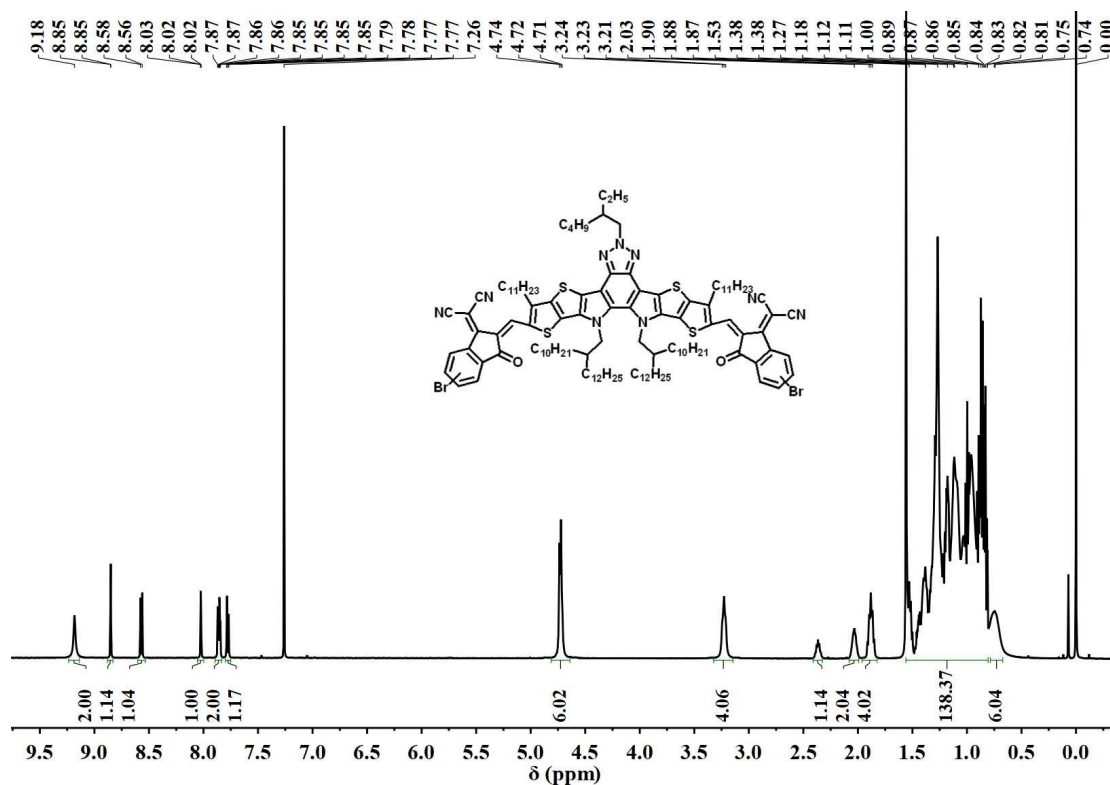


Fig. S11 ^1H NMR spectrum of compound TTPTAZ-ICBr in CDCl_3 .

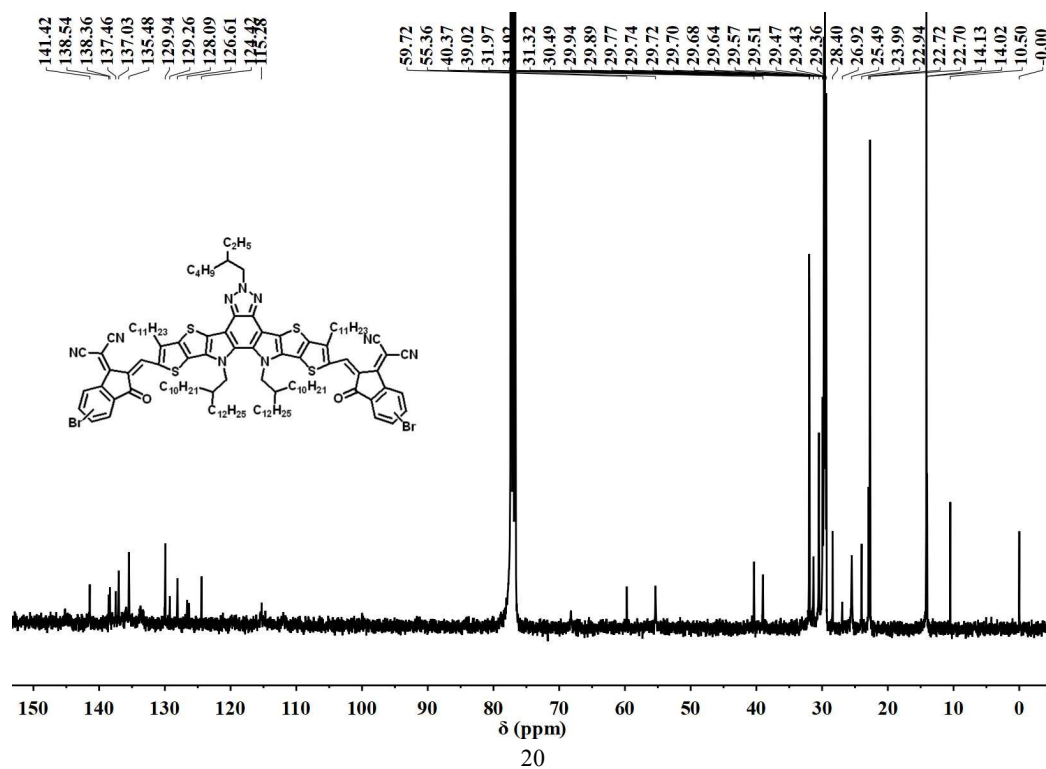


Fig. S12 ^{13}C NMR spectrum of compound TTPTAZ-ICBr in CDCl_3 .

References

- 1 J. Yuan, Y. Zhang, L. Zhou, G. Zhang, H.-L. Yip, T.-K. Lau, X. Lu, C. Zhu, H. Peng, P. A. Johnson, M. Leclerc, Y. Cao, J. Ulanski, Y. Li and Y. Zou, *Joule*, 2019, **3**, 1140.
- 2 J. Yuan, T. Huang, P. Cheng, Y. Zou, H. Zhang, J. L. Yang, S.-Y. Chang, Z. Zhang, W. Huang, R. Wang, D. Meng, F. Gao and Y. Yang, *Nat. Commun.*, 2019, **10**, 570.
- 3 Z. -G. Zhang, Y. Yang, J. Yao, L. Xue, S. Chen, X. Li, W. Morrison, C. Yang and Y. Li, *Angew. Chem., Int. Ed.*, 2017, **56**, 13503.
- 4 Y. Meng, J. Wu, X. Guo, W. Su, L. Zhu, J. Fang, Z.-G. Zhang, F. Liu, M. Zhang, T. P. Russell and Y. Li, *Sci. China Chem.*, 2019, **62**, 845.
- 5 J. Wu, Y. Meng, X. Guo, L. Zhu, F. Liu and M. Zhang, *J. Mater. Chem. A*, 2019, **7**, 16190.
- 6 H. Yao, F. Bai, H. Hu, L. Arunagiri, J. Zhang, Y. Chen, H. Yu, S. Chen, T. Liu, J. Y. L. Lai, Y. Zou, H. Ade and H. Yan, *ACS Energy Lett.*, 2019, **4**, 417.
- 7 Q. Fan, W. Su, S. Chen, W. Kim, X. Chen, B. Lee, T. Liu, U. A. Méndez-Romero, R. Ma, T. Yang, W. Zhuang, Y. Li, Y. Li, T.-S. Kim, L. Hou, C. Yang, H. Yan, D. Yu and E. Wang, *Joule*, 2020, **4**, 658.
- 8 H. Yao, L. K. Ma, H. Yu, J. Yu, P. C. Y. Chow, W. Xue, X. Zou, Y. Chen, J. Liang, L. Arunagiri, F. Gao, H. Sun, G. Zhang, W. Ma and H. Yan, *Adv. Energy Mater.*, 2020, **10**, 2001408.
- 9 A. Tang, J. Li, B. Zhang, J. Peng and E. Zhou, *ACS Macro Lett.*, 2020, **9**, 706.
- 10 Q. Fan, R. Ma, T. Liu, W. Su, W. Peng, M. Zhang, Z. Wang, X. Wen, Z. Cong, Z. Luo, L. Hou, F. Liu, W. Zhu, D. Yu, H. Yan and E. Wang, *Sol. RRL*, 2020, **4**, 2000142.

- 11 Q. Fan, W. Su, S. Chen, T. Liu, W. Zhuang, R. Ma, X. Wen, Z. Yin, Z. Luo, X. Guo, L. Hou, K. Moth-Poulsen, Y. Li, Z. Zhang, C. Yang, D. Yu, H. Yan, M. Zhang and E. Wang, *Angew. Chem., Int. Ed.*, 2020, **59**, 1.
- 12 T. Jia, J. Zhang, W. Zhong, Y. Liang, K. Zhang, S. Dong, L. Ying, F. Liu, X. Wang, F. Huang and Y. Cao, *Nano Energy*, 2020, **72**, 104718.
- 13 W. Wang, Q. Wu, R. Sun, J. Guo, Y. Wu, M. Shi, W. Yang, H. Li and J. Min, *Joule*, 2020, **4**, 1070.
- 14 Y. Wu, Q. Wu, W. Wang, R. Sun and J. Min, *Sol. RRL*, 2020, **4**, 2000409.
- 15 H. Sun, H. Yu, Y. Shi, J. Yu, Z. Peng, X. Zhang, B. Liu, J. Wang, R. Singh, J. Lee, Y. Li, Z. Wei, Q. Liao, Z. Kan, L. Ye, H. Yan, F. Gao and X. Guo, *Adv. Mater.*, 2020, **32**, 2004183.
- 16 J. Du, K. Hu, L. Meng, I. Angunawela, J. Zhang, S. Qin, A. Liebman-Pelaez, C. Zhu, Z. Zhang, H. Ade and Y. Li, *Angew. Chem., Int. Ed.*, 2020, **59**, 15181.
- 17 Z. Yin, Y. Wang, Q. Guo, L. Zhu, H. Liu, J. Fang, X. Guo, F. Liu, Z. Tang, M. Zhang and Y. Li, *J. Mater. Chem. C*, 2020, **8**, 16180.
- 18 Q. Fan, Q. An, Y. Lin, Y. Xia, Q. Li, M. Zhang, W. Su, W. Peng, C. Zhang, F. Liu, L. Hou, W. Zhu, D. Yu, M. Xiao, E. Moons, F. Zhang, T. D. Anthopoulos, O. Inganäs and E. Wang, *Energy Environ. Sci.*, 2020, **13**, 5017.
- 19 B. Fan, L. Ying, P. Zhu, F. Pan, F. Liu, J. Chen, F. Huang and Y. Cao, *Adv. Mater.*, 2017, **29**, 1703906.
- 20 N. B. Kolhe, D. K. Tran, H. Lee, D. Kuzuhara, N. Yoshimoto, T. Koganezawa and S. A. Jenekhe, *ACS Energy Lett.*, 2019, **4**, 1162.
- 21 Z. Li, L. Ying, P. Zhu, W. Zhong, N. Li, F. Liu, F. Huang and Y. Cao, *Energy Environ.*

Sci., 2019, **12**, 157.

22 L. Zhu, W. Zhong, C. Qiu, B. Lyu, Z. Zhou, M. Zhang, J. Song, J. Xu, J. Wang, J. Ali, W.

Feng, Z. Shi, X. Gu, L. Ying, Y. Zhang and F. Liu, *Adv. Mater.*, 2019, **31**, 1902899.

23 K. Feng, J. Huang, X. Zhang, Z. Wu, S. Shi, L. Thomsen, Y. Tian, H. Y. Woo, C. R.

McNeill and X. Guo, *Adv. Mater.*, 2020, **32**, 2001476.